Highly photoluminescent blue ionic Platinum-Based Emitters

Violeta Sicilia,*[a] Lorenzo Arnal [b], Andrés J. Chueca [b], Sara Fuertes,*[b], Azin Babaei [c], Ana María Igual Muñoz,[c] Michele Sessolo[c] and Henk J. Bolink[c]

a. *Departamento de Química Inorgánica, Escuela de Ingeniería y Arquitectura de Zaragoza, Instituto de Síntesis Química y Catálisis Homogénea (ISQCH), CSIC - Universidad de Zaragoza, Campus Río Ebro, Edificio Torres Quevedo, 50018, Zaragoza (Spain).E-mail: sicilia@unizar.es.*

b. *Departamento de Química Inorgánica, Facultad de Ciencias, Instituto de Síntesis Química y Catálisis Homogénea (ISQCH), CSIC - Universidad de Zaragoza, Pedro Cerbuna 12, 50009, Zaragoza (Spain)*

c. *Instituto de Ciencia Molecular, Universidad de Valencia, C/J. Beltran 2, 46980, ´ Paterna, Spain*

Abstract

New cycloplatinated N-heterocyclic carbene (NHC) compounds with chelate diphosphines (P^P) as ancillary ligands: [Pt(R-C^C*)(P^P)]PF$_6$ (R = H, P^P = dppm **1A**, dppe **2A**, dppbz **3A**; R = CN, P^P = dppm **1B**, dppe **2B**, dppbz **3B**) have been prepared from the corresponding starting material [{Pt(R-C^C*)(μ-Cl)}$_2$] (R = H, **A**, R = CN, **B**) and fully characterized. The new compound **A** has been prepared by a stepwise protocol. The photophysical properties of **1A-3A** and **1B-3B** have been widely studied and supported by the time-dependent-density functional theory (TD-DFT). These compounds show an efficient blue (dppe, dppbz) or cyan (dppm) emission in PMMA films (5%wt), with photoluminescence quantum yield (PLQY) ranging from 30% to 87%. This emission has been assigned mainly to transitions from ^{3}ILCT [π(NHC) → π*(NHC)] excited states with

some ^{3}LL'CT [π(NHC) $\rightarrow$ π*(P^P)] character. The electroluminescence of these materials in proof-of-concept solution processed OLEDs containing **3A** and **3B** as dopants was investigated. The CIE coordinates for devices based on **3A** (0.22, 0.41) and **3B** (0.24, 0.44) fit within the sky blue region.

Introduction

Organic light-emitting diodes (OLEDs) have experienced an enormous progress over the last three decades, eventually resulting in their commercialization as active pixels in flat panel displays. This success has been driven by a continuous and parallel development of both the devices structure and the organic semiconductors and emitters.[1] The light-emitting layer (EML) is one of the most crucial components to achieve high-efficiency electroluminescence. Since by using traditional fluorescent materials only 25% of the generated excitons can be harvested in a device, much of the success of this technology has been enabled through the development of phosphorescent heavy metal complexes as luminescent dopants. Phosphorescent organic light-emitting diodes (PhOLEDs), in which both singlet and triplet excitons can be harvested to reach theoretical internal quantum efficiency up to 100%, are capable of high efficiencies and high colour quality across the visible spectrum.[1-6] Despite the remarkable progress in this technology, the development of efficient and stable deep-blue emitters with long operational lifetime is still a challenge.[7] While blue-emitting cyclometalated iridium (III) complexes, such as [Ir(C^N)$_2$(LX)] (C^N = 2-arylpyridinate) have been the most largely studied for optoelectronics and lighting applications,[8-10] recently Pt(II) complexes have also demonstrated their potential in this type of applications.[3, 7, 11] Among them, complexes bearing didentated or tridentated cyclometalated N-heterocyclic carbenes have been shown as promising efficient and stable blue-phosphorescent emitters.[3, 7, 12-22] In these compounds, the strong metal-carbon bonds

raise the energy of the MC states hindering their photo- or thermal population and then increasing the emission quantum yield and avoiding degradation via bond-breaking processes.[20, 23] The use of didentate cyclometalated carbenes (C^C*) allows to tune the emission properties by changing the nature of both, the C^C* and the ancillary ligands. In this field high efficient blue-emitters have been reported by our group.[19-22] Those containing chelate diphosphines, such as [Pt (R-C^C*)(P^P)] PF$_6$ (R-C= Naph, R =CO$_2$Et, P^P: dppm (diphenylphosphinomethane), dppe (diphenylphosphinoethane), dppbz (1,2-diphenylphosphino-benzene) showed high photoluminescence quantum yields (PLQY) and stability and were proved as the active components in photo- and electroluminescent devices.[21]

OLEDs can be manufactured with either vacuum deposition or solution-processing techniques. The former method is suitable for small molecules that, generally, have better performance and longer stability due to the purity of the sublimated samples.[24-26] Vacuum deposition, however, requires accurate control on doping concentration and wastes lot of material thereby increasing the manufacturing costs.[27] Recent developments on solution-processable OLEDs based on small molecules have focused on optimizing efficiency while using simple processing techniques.[27] However, there are still limited examples, in particular for solution-processable OLEDs based on Pt(II) complexes.[25, 26, 28-40]

Within this perspective we decided to extend the family of [Pt(R-C^C*)(P^P)]PF$_6$ compounds by changing the C^C* group. As result, herein we report the synthesis and the structural properties of compounds [Pt (R-C^C*)(P^P)]PF$_6$ (R= H, P^P: dppm **1A**, dppe **2A**, dppbz **3A**; R = CN, P^P: dppm **1B**, dppe **2B**, dppbz **3B**). The photophysical and TD-DFT studies were also carried out, showing photoluminescence quantum yield ranging from 30% to 87%. The electroluminescence (EL) properties of compound **3B**, were

evaluated in simple solution-processable blue PhOLEDs. The low electroluminescence efficiency observed was attributed to the large barrier for the hole injection, introduced by the large ionization energy (IE) of the Pt(II) emitter. Compounds **1A-3A**, without an electron-withdrawing substituent in the metalated fragment were prepared to raise the energy of the HOMO and to reduce the IE of these kind of compounds, which required the synthesis of the starting complex [{Pt(HC^C*)(µ-Cl)}$_2$](**A**). Then, the electroluminescence of **3A** was measured in the same conditions of **3B** and compared one to another.

Experimental

Synthesis and characterization of [Pt(C^C*)(dppm)]PF$_6$ (1A). dppm (102.2 mg, 0.26 mmol) and KPF$_6$ (48.44 mg, 0.26 mmol) were added to a suspension of **A** (100 mg, 0.13 mmol) in acetone (30 mL) at r. t.. After 1 h of reaction, the solvent was removed under reduced pressure and the residue was treated with dichloromethane (40 mL). The suspension was filtered through Celite and the solvent was removed under reduced pressure. The residue was treated with diethyl ether, filtered, and washed with diethyl ether to give **1A** as a yellow solid. Yield: 217 mg, 95 %. Anal. Calcd for C$_{35}$H$_{31}$F$_6$N$_2$P$_3$Pt: C 47.68, H 3.54, N 3.18; found: C 47.66, H 3.80, N 3.32. ^{1}H NMR (400 MHz, CD$_2$Cl$_2$): $\delta =$ 7.80-7.70 (m, 8H, Ho, Ph), 7.62-7.46 (m, 12H, Hm, Hp,Ph), 7.45 (d, $^2J_{H2,3} = 1.8$, $^5J_{H2,P} =0.8$, 1H, H$_2$), 7.20 (m, 1H, H$_{10}$), 7.17-7.08 (m, 2H, H$_7$, H$_9$), 7.03 (m, 1H, H$_3$), 6.79 (tt, $^3J_{H9,8} =$ $^3J_{H8,7} = 7.6$, $^5J_{H,P} = 1.5$, 1H, H$_8$), 4.75 (m, 2H, CH$_2$, dppm), 3.23 (s, 3H, H$_4$). ^{13}C{^{1}H} NMR plus HMBC and HSQC (101 MHz, CD$_2$Cl$_2$): $\delta = 172.1$ (d, $^2J_{C,P} = 125.8$, C$_1$), 148.7 (s, C$_5$), 142.4 (d, $^2J_{C,P} = 103.5$, C$_6$), 140.0 (dd, $^3J_{C,P} = 11.4$, $^3J_{C,P} = 4.1$, C$_7$), 134.0 (m, 8C, Co), 133.1 (m, 4C, Cp), 130.2 (m, 8C, Cm), 128.3 (dd, $^1J_{C,P} = 40.7$, $^3J_{C,P} = 7.8$, 2C, Ci), 127.6 (m, 1C, C$_8$), 127.3 (s, 1C, C$_9$,), 126.5 (dd, $^1J_{C,P} = 48.4$, $^3J_{C,P} = 8.2$, 2C, Ci), 123.8 (d, $^4J_{C,P} = 5.5$, 1C, C$_3$), 116.4 (d, $^4J_{C,P} = 2.0$, 1C, C$_2$), 112.3 (d, $^4J_{C,P} = 3.6$, $^3J_{C,Pt} = 26.2$, 1C, C$_{10}$), 50.24 (t, $^1J_{C,P}$

= 30.1, 1C, CH_2, dppm), 38.9 (s, 1C, C_4). $^{31}P\{^1H\}$ NMR (162 MHz, CD_2Cl_2): δ = -37.8 (ν_A, $P_{trans-C1}$, $J_{Pt,P}$ = 2401.9, $J_{P,P}$ = 39.8), -38.5 (ν_B, $P_{trans-C6}$, $J_{Pt,P}$ = 1515.6). $^{195}Pt\{^1H\}$ NMR (86 MHz, CD_2Cl_2): δ = -4389.9 (dd). IR (cm^{-1}): ν = 830, 545 (s, PF_6). MS (MALDI+): m/z (100) 736.0 $[M]^+$. Λ_M ($5 \cdot 10^{-4}$ M acetone solution): 64.8 Ω^{-1} cm^2 mol^{-1}.

Synthesis and characterization of [Pt(C^C*)(dppe)]PF$_6$ (2A). It was prepared following the method described for **1A** with dppe (106.0 mg, 0.26 mmol), KPF_6 (48.4 mg, 0.26 mmol) and **A** (100.0 mg, 0.13 mmol) (2 h). **2A** was obtained as a pale yellow solid (Yield: 215 mg, 93 %). Anal. Calcd for $C_{36}H_{33}F_6N_2P_3Pt$: C 48.28, H 3.71, N 3.13; found: C 48.11, H 3.80, N 3.36. ^1H NMR (400 MHz, CD_2Cl_2): δ = 8.00-7.84 (m, 8H, Ho, Ph), 7.68-7.48 (m, 13H, Hm, Hp,Ph, H_2), 7.24 (m, 1H, H_{10}), 7.17 (m, 1H, H_7), 7.10 (td, $^3J_{H9,8}$ = $^3J_{H9,10}$ = 7.5, $^4J_{H9,7}$ = 0.8, 1H, H_9), 6.97 (m, 1H, H_3), 6.64 (tt, $^3J_{H9,8}$ = $^3J_{H8,7}$ = 7.6, $^5J_{H,P}$ = 1.4, 1H, H_8), 3.03 (s, 3H, H_4), 2.34 (m, 4H, CH_2, dppe). $^{13}C\{^1H\}$ NMR plus HMBC and HSQC (101 MHz, CD_2Cl_2): δ = 172.7 (dd, $^2J_{C,P}$ = 128.7, $^2J_{C,P}$ = 7.4, C_1), 148.3 (s, C_5), 143.7 (dd, $^2J_{C,P}$ = 103.1, $^2J_{C,P}$ = 5.9, C_6), 140.7 (dd, $^3J_{C,P}$ = 10.1, $^3J_{C,P}$ = 1.5, $^1J_{C,Pt}$ = 50.1, C_7), 134.7 (d, $^2J_{C,P}$ = 12.2, 4C, Co), 134.2 (m, $^2J_{C,P}$ = 12.6, 4C, Co), 133.2 (d, $^4J_{C,P}$ = 2.0, 2C, Cp), 133.0 (d, $^4J_{C,P}$ = 2.0, 2C, Cp), 130.4 (d, $^3J_{C,P}$ = 10.9, 4C, Cm), 130.0 (d, $^3J_{C,P}$ = 11.4, 4C, Cm), 129.2 (d, $^1J_{C,P}$ = 46.6, 2C, Ci), 127.3 (d, $^1J_{C,P}$ = 54.1, 2C, Ci), 127.3 (dd, $^4J_{C,P}$ = 7.2, $^4J_{C,P}$ = 2.5, 1C, C_8), 127.0 (s, 1C, C_9,), 124.6 (d, $^4J_{C,P}$ = 4.5, 1C, C_3), 116.4 (d, $^4J_{C,P}$ = 2.2, 1C, C_2), 112.2 (d, $^4J_{C,P}$ = 3.4, $^3J_{C,Pt}$ = 24.8, 1C, C_{10}), 39.4 (s, 1C, C_4), 32.1(m, CH_2 dppe). $^{31}P\{^1H\}$ NMR (162 MHz, CD_2Cl_2): δ = 50.6 (d, $P_{trans-C1}$, $J_{Pt,P}$ = 2728.6, $J_{P,P}$ = 6), 43.5 (d, $P_{trans-C6}$, $J_{Pt,P}$ = 1919.2). $^{195}Pt\{^1H\}$ NMR (86 MHz, CD_2Cl_2): δ = -4990.0 (dd). IR (cm^{-1}): ν = 830, 545 (s, PF_6). MS (MALDI+): m/z (100) 750.0 $[M]^+$. Λ_M ($5 \cdot 10^{-4}$ M acetone solution): 67.8 Ω^{-1} cm^2 mol^{-1}.

Synthesis and characterization of [Pt(C^C*)(dppbz)]PF$_6$ (3A). It was prepared following the method described for **1A** with dppbz (110.9 mg, 0.24 mmol), KPF$_6$ (45.7 mg, 0.24 mmol) and **A** (94.4 mg, 0.12 mmol) (3 h). **3A** was obtained as a pale yellow solid (Yield: 210.5 mg, 92 %). Anal. Calcd for C$_{40}$H$_{33}$F$_6$N$_2$P$_3$Pt: C 50.91, H 3.52, N 2.97; found: C 50.54, H 3.57, N 2.60. ^{1}H NMR (400 MHz, CD$_2$Cl$_2$): δ = 7.86-7.77 (m, 4H, Ho, Ph), 7.69-7.60 (m, 4H, Ho, Ph), 7.60-7.37 (m, 17H, Hm, Hp, Ph, H$_a$, H$_b$, H$_c$, H$_d$, H$_2$), 7.29- 7.20 (m, 2H, H$_7$, H$_{10}$), 7.13 (td, $^3J_{H9,8}$ = $^3J_{H9,10}$ =7.6, $^4J_{H9,7}$ = 0.9, 1H, H$_9$), 6.95 (m, 1H, H$_3$), 6.68 (tt, $^3J_{H9,8}$ = $^3J_{H8,7}$ = 7.5, $^5J_{H,P}$ = 1.4, 1H, H$_8$), 3.03 (s, 3H, H$_4$). ^{13}C{^{1}H} NMR plus HMBC and HSQC (101 MHz, CD$_2$Cl$_2$): δ = 172.6 (1C, C$_1$), 148.2 (s, 1C, C$_5$), 143.7 (1C, C$_6$), 140.2 (dd, $^3J_{C,P}$ = 9.3, $^3J_{C,P}$ = 2.4, $^2J_{C,Pt}$ = 50.3, 1C, C$_7$), 134.4 (m, 8C, Co), 133.7-133.2 (m, 4C, C$_a$, C$_b$, C$_c$, C$_d$), 132.8 (d, $^4J_{C,P}$ = 2.2, 2C, Cp), 132.6 (d, $^4J_{C,P}$ = 2.2, 2C, Cp), 130.2 (d, $^3J_{C,P}$ = 11.0, 4C, Cm), 129.8 (d, $^3J_{C,P}$ = 11.5, 4C, Cm), 128.2 (d, $^2J_{C,P}$ = 58.2, 4C, Ci), 127.1 (m, 2C, C$_9$, C$_8$), 124.7 (d, $^4J_{C,P}$ = 4.5, 1C, C$_3$), 116.5 (1C, C$_2$), 112.3 (d, $^4J_{C,P}$ = 3.3, $^3J_{C,Pt}$ = 25.8, 1C, C$_{10}$), 39.3 (1C, C$_4$). ^{31}P{^{1}H} NMR (162 MHz, CD$_2$Cl$_2$): δ = 47.3 (d, P$_{trans-C1}$, $J_{Pt,P}$ = 2683.5, $J_{P,P}$ = 4.1), 39.9 (d, P$_{trans-C6}$, $J_{Pt,P}$ = 1909.1). ^{195}Pt{^{1}H} NMR (86 MHz, CD$_2$Cl$_2$): δ = -4940.2 (dd). IR (cm^{-1}): ν = 830, 545 (s, PF$_6$). MS (MALDI+): m/z (100) 798.1 [M]$^+$. Λ_M (5·10^{-4} M acetone solution): 68.4 Ω^{-1} cm^2 mol^{-1}.

Synthesis and characterization of [Pt(NC-C^C*)(dppm)]PF$_6$ (1B). It was prepared following the method described for **1A** with dppm (115.4 mg, 0.29 mmol), KPF$_6$ (54.7 mg, 0.29 mmol) and **B**^{41} (120.2 mg, 0.15 mmol) (3 h). **1B** was obtained as a white solid (Yield: 246.1 mg, 93 %). Anal. Calcd for C$_{36}$H$_{30}$F$_6$N$_3$P$_3$Pt: C 47.69, H 3.34, N 4.63; found: C 48.02, H 3.13, N 4.52. ^{1}H NMR (400 MHz, CD$_2$Cl$_2$,): δ = 7.79-7.69 (m, 8H, Ho, Ph), 7.64-7.50 (m, 13H, H$_2$ and Hm, Hp, Ph), 7.47 (dd, $^3J_{H9,10}$ = 8.1, $^4J_{H9,7}$ = 1.6, 1H, H$_9$), 7.31 (dd,

$^3J_{H10,9}$ = 8.1, $^5J_{H10,P}$ = 2.1, 1H, H$_{10}$), 7.25 (m, $^3J_{H7,Pt}$ = 57.9, 1H, H$_7$), 7.12 (m, 1H, H$_3$), 4.89-4.68 (m, 2H, CH$_2$ (dppm)), 3.24 (s, 3H, H$_4$). ^{13}C{^{1}H} NMR plus HMBC and HSQC (101 MHz, CD$_2$Cl$_2$): δ = 172.2 (C$_1$), 152.0 (s, C$_5$), 142.4 (dd, $^3J_{C,P}$= 11.0; $^3J_{C,P}$= 5.0, C$_7$), 134.1 (d, $^2J_{C,P}$ = 12.0, 4C, Co (dppm)), 133.8 (d, $^2J_{C,P}$ = 12.3, 4C, Co (dppm)), 133.5 (d, $^4J_{C,P}$ = 2.4, 2C, Cp (dppm)), 133.4 (d, $^4J_{C,P}$ = 2.3, 2C, Cp (dppm)), 132.2 (s, C$_9$), 130.5 (d, $^3J_{C-P}$ = 11.0, 4C, Cm (dppm)), 130.3 (d, $^3J_{C,P}$ = 11.4, 4C, Cm (dppm)), 127.6 (dd, $^2J_{C,P}$ = 41.2, $^2J_{C,P}$ = 9.3, Ci (dppm)), 125.6 (dd, $^2J_{C,P}$ = 47.2, $^2J_{C,P}$ = 9.9, Ci (dppm)), 124.7 (d, $^4J_{C3,P}$ = 4.3, C$_3$), 119.2 (s, CN), 116.9 (d, $^4J_{C2,P}$ = 2.0, $^3J_{C3,Pt}$ = 35.7, C$_2$), 112.6 (d, $^4J_{C10,P}$ = 3.1, $^3J_{C10,Pt}$ = 25.6, C$_{10}$), 110.7 (m, C$_8$), 49.8 (dd, $^1J_{C,P}$ = 31.2, $^1J_{C,P}$ = 29.4, CH$_2$ (dppm)), 39.1 (dd, $^4J_{C,P}$ = 3.8, $^4J_{C,P}$ = 1.9, C$_4$). ^{31}P{^{1}H} NMR (162 MHz, CD$_2$Cl$_2$): δ = -38.5 (ν$_A$, P$_{trans-C1,}$ $J_{Pt,P}$ = 2345.3, $J_{P,P}$ = 44.0), -39.0 (ν$_B$, P$_{trans-C6}$, $J_{Pt,P}$ = 1611.9). ^{195}Pt{^{1}H} NMR (86 MHz, CD$_2$Cl$_2$): δ = -4426.7 (dd).   IR (cm^{-1}): ν = 2219 (m, CN), 833 (s, PF$_6$), 555 (s, PF$_6$). MS (MALDI+): m/z (100) 761.1 [M]$^+$. Λ$_M$ (5·10^{-4} M acetone solution): 65.3 Ω^{-1} cm^2 mol^{-1}.

Synthesis and characterization of [Pt(NC-C^C*)(dppe)]PF$_6$ (2B). This complex was prepared similarly to **2A**, as was described in the Literature.[41] ^{31}P{^{1}H} NMR (162 MHz, CD$_2$Cl$_2$): δ = 50.2 (d, P$_{trans-C1}$, $J_{Pt,P}$ = 2673.8, $J_{P,P}$ = 7.0), 43.1 (d, P$_{trans-C6}$, $J_{Pt,P}$ = 2014.6). ^{195}Pt{^{1}H} NMR (86 MHz, CD$_2$Cl$_2$): δ = -4996.0 (dd).

Synthesis and characterization of [Pt(NC-C^C*)(dppbz)]PF$_6$ (3B). It was prepared following the method described for **1A** dppbz (130.0 mg, 0.29 mmol), KPF$_6$ (54.6 mg, 0.29 mmol) and **B**[41] (120.0 mg, 0.14 mmol) (3 h). **3B** was obtained as a white solid (Yield: 261.9 mg, 93 %). Anal. Calcd for C$_{41}$H$_{32}$F$_6$N$_3$P$_3$Pt: C 50.83, H 3.33, N 4.34; found: C 51.21, H 3.32, N 4.05. ^{1}H NMR (400 MHz, CD$_2$Cl$_2$, δ): 7.82-7.73 (m, 4H, Ho, Ph), 7.64-7.37 (m, 22H, H$_2$, H$_9$, H$_a$, H$_b$, H$_c$, H$_d$, Ho, Hm and Hp, Ph), 7.37-7.24 (m, 2H, H$_7$ and H$_{10}$),

7.02 (m, 1H, H$_3$), 3.03 (s, 3H, H$_4$). ^{13}C{^{1}H} NMR plus HMBC and HSQC (101 MHz, CD$_2$Cl$_2$): δ = 173.0 (dd, $^2J_{C1,P}$= 129.3; $^2J_{C1,P}$ = 7.1, 1C, C$_1$), 151.6 (s, 1C, C$_5$), 144.4 (dd, $^2J_{C6,P}$= 105.4, $^2J_{C1,P}$= 5.7, 1C, C$_6$), 142.9 (dd, $^3J_{C7,P}$= 9.0; $^3J_{C7,P}$= 3.3, $^2J_{C7,Pt}$ = 52.5, 1C, C$_7$), 134.5 (d, $^2J_{C,P}$ = 10.7, 4C, Co), 134.4 (d, $^2J_{C,P}$ = 11.6, 4C, Co), 133.0 (s, br, 4C, Cp), 130.3 (d, $^3J_{C,P}$ = 11.1, 4C, Cm), 130.4 (d, $^3J_{C,P}$ = 11.5, 4C, Cm), 134.1-133.9 (m, C$_{Ar}$ (dppbz)), 133.6-133.3 (m, C$_{Ar}$ (dppbz)), 131.6 (s, 1C, C$_9$), 125.5 (d, $^4J_{C3,P}$ = 4.6, $^3J_{C3,Pt}$ = 29.7, 1C, C$_3$), 118.5 (s, CN), 117.1 (d, $^4J_{C2,P}$ = 2.1, $^3J_{C3,Pt}$ = 34.6, C$_2$), 112.6 (d, $^4J_{C10,P}$ = 3.3, $^3J_{C10,Pt}$ = 25.2, C$_{10}$), 110.7 (m, C$_8$), 39.4 (s, C$_4$). ^{31}P{^{1}H} NMR (162 MHz, CD$_2$Cl$_2$): δ = 46.4 (d, P$_{trans-C1}$, $J_{Pt,P}$ = 2634.7, $J_{P,P}$ = 5.2), 39.3 (d, P$_{trans-C6}$, $J_{Pt,P}$ = 2001.4). ^{195}Pt{^{1}H} NMR (86 MHz, CD$_2$Cl$_2$): δ = -4939.6 (dd). IR (cm^{-1}): ν = 2222 (m, CN), 831 (s, PF$_6$), 546 (s, PF$_6$). MS (MALDI+): m/z (100) 823.2 [M]$^+$. Λ_M (5·10^{-4} M acetone solution): 64.9 Ω^{-1} cm^2 mol^{-1}.

Results and discussion

Synthesis and Characterization

Compounds [Pt(R-C^C*)(P^P)]PF$_6$ (**1A- 3A**; **1B- 3B,** see Scheme 1) were prepared in high yields, 90% – 95%, from the corresponding starting compound, **A** or **B**, following the same procedure that the previously reported one.[21] This synthetic procedure requires the availability of the dichloro bridged complexes **A** and **B**. Therefore we prepared the new compound **A** by an step-by-step method, similar to that described previously for the synthesis of **B**[41] (see SI part 1.6 for experimental details and Figures S1-S2 for NMR spectra). Relevant structural information for the characterization of **1A-3A** and **1B-3B** came from multinuclear NMR spectra (see Table 1, Experimental section and Figures S3-S8 in SI).

R= H, **A**   R= H, P^P = dppm (**1A**), dppe (**2A**) dppbz (**3A**)
R= CN, **B** R= -CN, P^P = dppm (**1B**), dppe (**2B**) dppbz (**3B**)
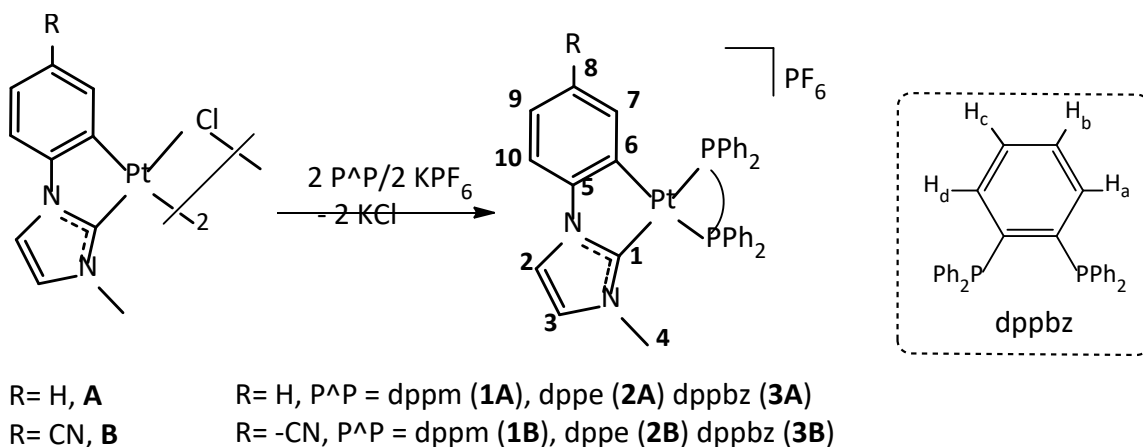
Scheme 1: Synthesis of new complexes and numeration scheme for NMR characterization

The chemical shifts of the ^{195}Pt and those of the two inequivalent P atoms, the $J_{P,P}$ values and the $^1J_{Pt,P}$ ones are in agreement with the proposed structure and are similar to those found in the related compounds [Pt(CO$_2$Et-C^C*)(P^P)]PF$_6$ (P^P = dppm, dppe, dppbz).[21] From these data we can see that the presence of an electron withdrawing substituent (CN) in the metalated aryl fragment causes the increase of the $J_{P,P}$ and the $J_{Pt,Ptrans-C6}$ at the same time that the decrease of the $J_{Pt,Ptrans-C1}$.

Table 1: Relevant ^{31}P{^{1}H}[a] and ^{195}Pt{^{1}H}[b] NMR data (δ(ppm), J(Hz))

	δ Pt	$J_{Pt,Ptrans-C1}$	$J_{Pt,Ptrans-C6}$	δP$_{trans-C1}$	δP$_{trans-C6}$	$J_{P,P}$
1A	-4389.9	2401.9	1515.6	-37.8v_A	-38.5 v_B	39.8
2A	-4990.0	2728.6	1919.2	50.6	43.5	6.0
3A	-4940.2	2683.5	1909.1	47.3	39.9	4.1
1B	-4426.7	2345.3	1611.9	-38.5v_A	-39.0v_B	44.0
2B	-4996.0	2673.8	2014.6	50.2	43.1	7.0
3B	-4939.6	2634.7	2001.4	46.4	39.3	5.2

[a] 162 MHz, CD$_2$Cl$_2$; [b] 86 MHz, CD$_2$Cl$_2$

The X-ray diffraction study on single crystals of **1A**, **1B** and **3B** confirmed the proposed structure for these cations (see Tables 2 and S1, Figures 1 and S9).
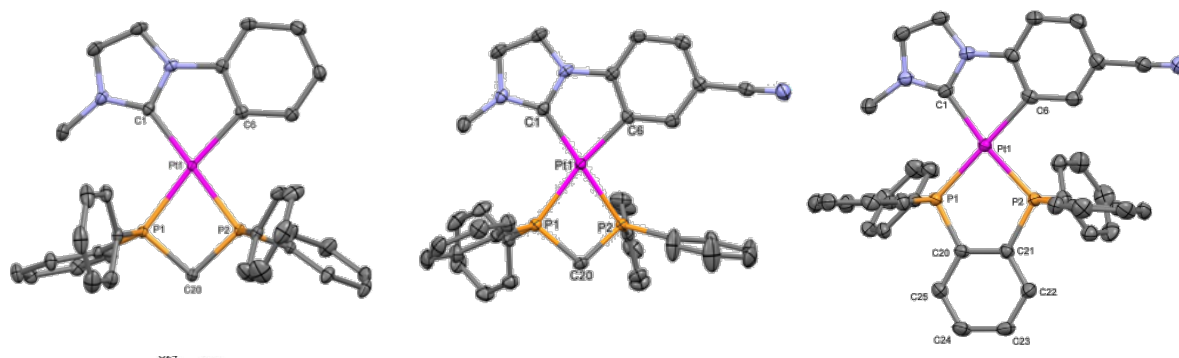
Figure 1. Molecular structures of the cationic complexes for **1A** (left), **1B** (middle) and **3B** (right). Thermal ellipsoids are drawn at the 50% probability level. Hydrogen atoms, PF_6 and solvent molecules have been omitted for clarity.

In all of these complexes the platinum center exhibits a distorted square-planar environment as a consequence of the small bite angles of both chelate ligands (R-C^C* and P^P, especially when P^P is dppm). As can be seen in Table 2, bond distances and angles concerning the "Pt(C^C*)" moiety are similar to those observed for other five-membered metalacycles of Pt(II) with the N-heterocyclic carbenes.[18, 41-44] Regarding the "Pt(P^P)" fragment, the Pt–P1 bond lengths are slightly longer than those of the Pt-P2 ones, complying with the C6 atom having a higher *trans* influence than that of the C1 atom.[41] In the cation complexes of **3B** (two molecules crystallize in the asymmetric unit) the benzene ring (C20-C25) are not coplanar with the Pt (II) coordination plane (Pt, C1, C6, P1, P2), forming a dihedral angle of 19.0º and 15.9°, respectively. In their crystal structure packings, there are no Pt-Pt contacts. However, rather weak intermolecular interactions were observed. The molecules arrange themselves in pairs in a head-to-tail fashion supported by π⋯π (3.49 – 3.37 Å in **1B**, 3.60- 3.68 Å in **1A**) intermolecular contacts between the C^C* fragments, (see Figure S9). Also, there are some weak C-H⋯F contacts (d C-F= 2.97 - 3.42

Å; d H-F= 2.33 - 2.85 Å) between the complex cation and the PF_6^- anion (see Figure S9).[45-47]

Table 2: Selected bond lengths (Å) and angles (°).

	1A·Me₂CO	1B	3B·0.5 CH₂Cl₂
Pt(1)-C(1)	2.033(2)	2.041(3)	2.064(4)/ 2.067(4)
Pt(1)-C(6)	2.058(2)	2.054(3)	2.090(4)/ 2.099(4)
Pt(1)-P(1)	2.323(1)	2.328(1)	2.304(1)/ 2.305(1)
Pt(1)-P(2)	2.294(1)	2.292(1)	2.276(1)/ 2.273(1)
C(1)-Pt(1)-C(6)	79.3(1)	79.4(1)	79.3(2)/ 79.1(2)
C(6)-Pt(1)-P(2)	101.5(1)	100.3(1)	95.1(1)/ 94.6(1)
C(1)-Pt(1)-P(1)	107.0(1)	109.3(1)	101.2(1)/ 102.0(1)
P(1)-Pt(1)-P(2)	71.9(1)	71.2(1)	84.5(1)/ 84.3(1)

Some degree of cation-anion association seems to occur in acetone solutions, which substantiates the low conductivity values observed for them (Λ_M: 64.8- 68.4 Ω^{-1} cm^2 mol^{-1} in a 5x10^{-4} M) compared with the expected ones (100-120 Ω^{-1} cm^2 mol^{-1}) in acetone solution.[48]

Photophysical Properties and Theoretical Calculations

Absorption properties and TD-DFT calculations. The lowest energy absorption of **1B–3B** in CH₂Cl₂ (5·10^{-5} M) appear at λ ~ 320 nm, at higher energies than those of **1A-3A** (*ca*. 330 nm, Figure 2 and Table S2 in SI, part 4), which could be justified by the presence of an electron withdrawing substituent (CN) in the metalated aryl fragment. On the other hand, the low energy bands of the dppm derivatives (**1A** and **1B**) appear red shifted with

respect to the corresponding dppe and dppbz ones (**2A**, **2B** and **3A, 3B**), indicating that both, R-C^C* and P^P ligands are involved in the lowest energy spin-allowed transition. These absorptions obey the Beer's law in the range 5×10^{-4} M – 1×10^{-6} M in CH_2Cl_2 in agreement with the absence of significant aggregation in this concentration range (see Figure S10 in SI part 4).[6]

Theoretical calculations (DFT and TD-DFT) were carried out on the cations of **1A/B** and **3A/B** (see SI part 5 for Tables S3-S8, Figures S11-S14 and discussion). The calculated spin-allowed transition (S_1) of each complex fits well with its lowest energy absorption and they follow the experimental trend. Analysis of the frontier molecular orbitals (FOs) in the ground state showed that the presence of the electron withdrawing substituent, CN, in the metalated aryl fragment of complexes **B**, stabilize both, the HOMO and LUMO, but in different degree, with respect to those in complexes **A**, leading to a subtle shift to higher energies of their S_1 transition.
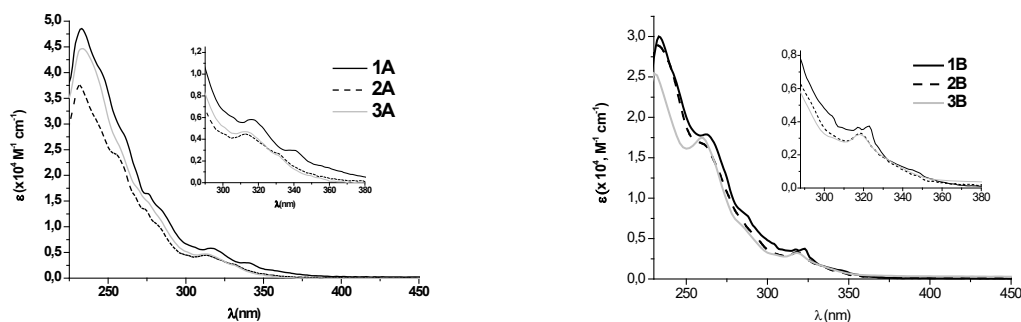
Figure 2.UV-VIS absorption spectra of **1A–3A** (left) and **1B–3B** (right) in CH_2Cl_2 (5×10^{-5} M). Insets: expanded views of the lower-energy absorptions

Considering that the main contribution to S_1 (91-96%) is the HOMO to LUMO transition, the origin of this absorption is mainly LL'CT [π(NHC) → π*(P^P)]/ILCT [π(NHC) → π*(NHC)] in nature with some LMCT [π(NHC) → 5d(Pt)] character in the case of the **A** derivatives (**1A** and **3A**).

Emission properties. Emission data for **1A–3A** and **1B–3B** are summarized in Table S9 (SI part 6). At room temperature in CH_2Cl_2 solution these compounds are scarcely luminescent, even in an argon atmosphere; population of dd* states or formation of exciplexes are very common thermal quenching processes for discrete blue-emitting Pt(II) complexes.[17, 22] Therefore we paid attention on their luminescence in rigid matrix of CH_2Cl_2 (10^{-5} M; 77 K), in poly(methyl methacrylate) (PMMA) films (5% wt doped) or in solid state. In these conditions, compounds **1A–3A** and **1B–3B** show a bright blue phosphorescent emission, with maxima at $\lambda \sim 450$ nm for the dppe and dppbz derivatives and 460 nm for the dppm ones, and a structured shape, with vibronic spacings (~ 1474 cm^{-1}) corresponding to the C=C/ C=N stretches of the cyclometalated NHC ligands (see Figure 3 for **3A** and **1B** and Figure S15). The emissive properties resulted to be similar to those for analogous compounds.[21]

On the light of the spectral profiles, the long decay times and the TD-DFT calculations, these phosphorescent emissions can be assigned mainly to transitions from ^{3}ILCT [π(NHC) $\rightarrow \pi$*(NHC)] excited states with some ^{3}LL'CT [π(NHC) $\rightarrow \pi$*(P^P)] character considering the subtle shift of the emission depending on the P^P ligand.
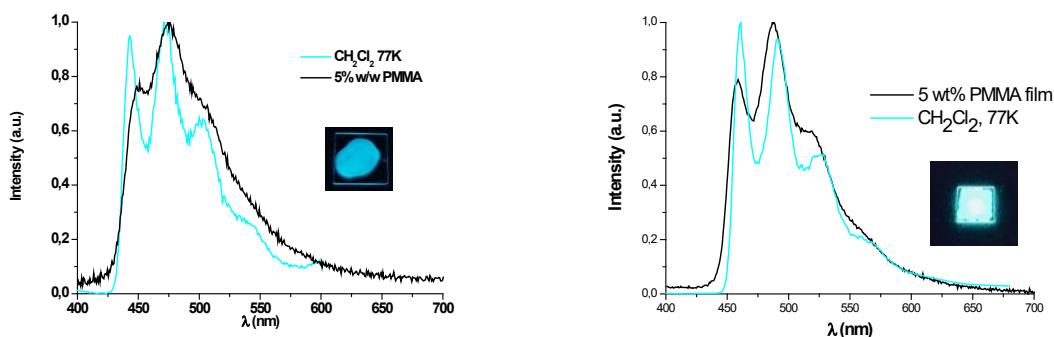
Figure 3. Normalized emission spectra of **3A** (left) and **1B** (right). Pictures were taken under 365 nm- UV light.

This assignment is in agreement with the large singlet-triplet splitting values ($\Delta E_{S,T} \sim 1$ eV, see Table S9)[49, 50] and the calculated radiative rate constants at r.t. ($k_r = \Phi_{PL}/\tau$), which are in the order of 10^4 s^{-1} for the emission in PMMA films. PLQY (Φ) measurements in PMMA films revealed that all complexes are good emitters at room temperature, especially the NC-C^C* derivatives (**1B-3B**). The PLQY values range from 30% to 57% for **1A-3A** while range from 75% to 87% for **1B-3B** under argon atmosphere (see Table S9), being amongst the most efficient blue and green-cyan emitters of platinum(II) in PMMA film: NBu$_4$[Pt(C^C*)(CN)$_2$] ($\Phi = 0.17$- 0.70),[22] [Pt(C^C*)(P^P)]PF$_6$ ($\Phi = 0.53$- 0.95),[21] [Pt(C^C*)(acac)] ($\Phi = 0.86$,[18] 0.90),[44] [Pt(C*^C^C*)Cl] ($\Phi = 0.32$),[51] and [Pt(C^X-L^L')] [C^X = phenyl methyl imidazole; L^L' = phenoxy pyridine, $\Phi = 0.58$; L^L' = carbazolyl pyridine, $\Phi = 0.89$; C^X = phenyl pyrazole; L^L' = carbazolyl pyridine, $\Phi = 0.85$].[52]

In the solid state, the PLQY, measured in the air, show an important decrease with respect to those in PMMA under Ar atmosphere. The quenching of the phosphorescence could be attributed to the contact with dioxygen and to secondary interactions among molecules derived from the solid state. The effect of the P^P ligand in the emission colour is easily perceptible in the CIE 1931 chromaticity diagram (Figure S16),with those complexes bearing dppm lying on the cyan region while the other on the blue one.

Solution-processed OLEDs using 3A and 3B as emitters

In view of the high photoluminescence quantum efficiency and stability of these compounds, we studied their properties when used as emitting centres in solution-processed multilayer OLEDs. The compounds [Pt(R-C^C*)(dppbz)]PF$_6$ (R = H, **3A**, R = CN, **3B**) were chosen as blue emitters due to their high PLQY and as representatives of the two

materials families. Details of the device fabrication are reported in the SI. Briefly, OLEDs were prepared on indium tin oxide (ITO) coated glass substrates. A thin (40 nm) layer of poly(3,4-ethylenedioxythiophene) polystyrene sulfonate (PEDOT:PSS) was used as the hole injection layer (HIL), to enlarge the work function and flatten the ITO electrode. The EML (30 nm thick) was spin-coated from solutions of the host, 4,4'-Bis(carbazol-9-yl)biphenyl (CBP), containing 20 wt.% of the Pt(II) complex. CBP was used because of its deep HOMO, close in energy with respect to the emitters used here.[53]
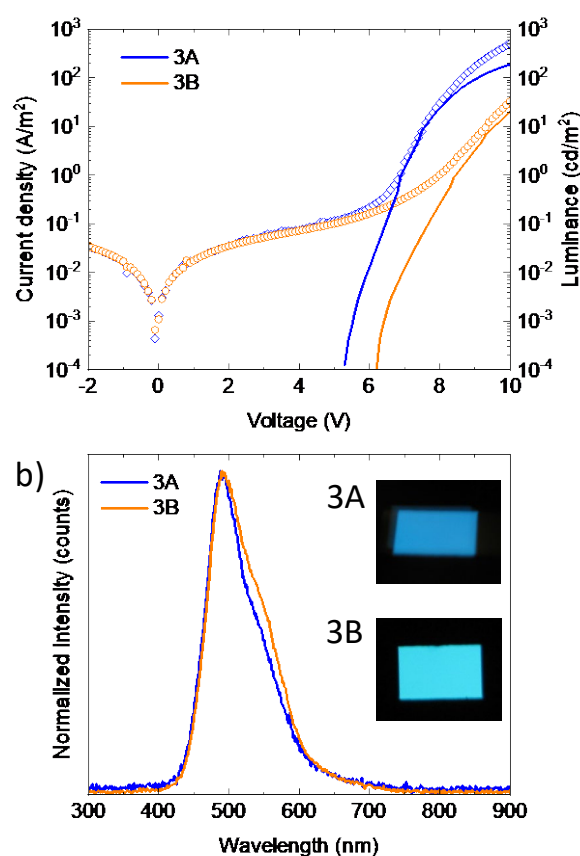
Figure 4. a) JVL characteristics for OLEDs employing **3A** and **3B** as the emitters. b) Electroluminescence spectra collected from the same devices, the inset shows pictures of working pixels.

The devices were finished by vacuum deposition of a 30 nm thick electron transport layer (ETL, 1,3-Bis[3,5-di(pyridin-3-yl)phenyl]benzene, BmPyPhB) and a bilayer cathode composed of lithium quinolate (Liq, 2 nm) and silver (100 nm).

Figure 4a shows the current density and luminance vs. voltage (JVL) curves registered for the OLEDs employing either **3A** or **3B** as the emitting material. The current density at low voltage is identical for the two devices, but we observed a steeper current injection at about 6V for the device with the **3A** compound. At 10 V applied bias, the current density for the **3A** OLEDs reached approximately 500 A/m^2, while it was limited to only 30 A/m^2 for the device with the **3B** compound.

Electroluminescence was also detected at high bias, at approximately 5 and 6 V for the OLEDs employing **3A** and **3B** respectively. The maximum luminance measured at 10 V was 200 cd/m^2 in the case of **3A**, while the device with **3B** showed weaker electroluminescence, about 20 cd/m^2. The electroluminescence spectra are shown in Figure 4b, and fall within the blue-cyan region of the electromagnetic spectrum (see CIE diagram in Figure S17) as expected from the photoluminescence characterization described above. The overall current efficiency at the maximum luminance are rather moderate, 0.4 and 0.7 cd/A when using **3A** or **3B**, respectively.

Among the possible reasons for the low electroluminescence efficiency, one can be the rather low current density and especially the large voltage required to observe charge injection within the device. In order to shed light on this phenomenon, we measured by air photoemission spectroscopy (Figure S18) the ionization energy (IE) of the two compounds, and found that IE = 5.7 eV and 6.0 eV for the **3A** and **3B**, respectively. The larger IE for **3B** is related with the electron withdrawing character of the substituent (CN), which stabilizes

the HOMO of the complex, as described above. In both cases, the HOMO level is rather deep, and could prevent an efficient hole injection/transport even though the materials are mixed with an organic semiconducting host. The fact the IE is smaller for the **3A** compound correlates with the higher current density flowing through the device and hence with the more intense electroluminescence efficiency. In spite of the moderate luminance of these solution-processed OLEDs, still, complex **3A** leads to a brighter electroluminescence than that of analogous blue emitting solution processed Pt OLEDs.[20] Besides, it is worth to note that the CIE coordinates of devices based on **3A** (0.22, 0.41) and **3B** (0.24, 0.44) fit within the sky blue region, unlike others solution-processed platinum-based PhOLEDs reported up to now.[25, 28, 30, 31, 34-36, 39]

Conclusions

New cycloplatinated NHC compounds with chelate diphosphines (P^P) as ancillary ligands, [Pt(R-C^C*)(P^P)]PF$_6$ (R = H, NC; P^P = dppm, dppe, dppbz) were prepared from their corresponding starting materials, [{Pt(R-C^C*)(μ-Cl)}$_2$]. The presence of two chelate ligands (C^C* and P^P) in these complexes confer them great robustness and thermal stability. Solution-processed OLEDs using **3A** and **3B** as emitters displayed moderate but sky-blue emissions. Importantly, we found larger current densities and higher luminescence for the OLEDs employing the **3A** emitter, whose ionization energy is 0.3 eV smaller as compared to the **3B** compound. The absence of an electron-withdrawing substituent in the metalated fragment of **3A** raises the HOMO's energy compared to that for **3B**. Most likely, the shallower HOMO in **3A** reduces the energy barrier present at the HIL/EML interface, which is hindering an efficient hole injection and limiting the device efficiency. Future studies will address this issue, tuning the frontier orbitals by appropriate changes in both, N-heterocyclic carbene and ancillary ligand.

ASSOCIATED CONTENT

Supporting Information

The Supporting Information is available free of charge on the ACS Publications website.

General information about experiments, instrumentation, X-ray crystallography, computational methods, preparation of the PMMA films, OLEDs fabrication and synthesis and characterization of the starting complex **A**. NMR figures for characterization; absorption and emission data; TD-DFT studies. CCDC: 1944541-1944543.

ACKNOWLEDGEMENTS

References

1.   Zhang, Q.-C.; Xiao, H.; Zhang, X.; Xu, L.-J.; Chen, Z.-N., Luminescent Oligonuclear Metal Complexes and the Use in Organic Light-Emitting Diodes. *Coord. Chem. Rev.* **2019,** *378*, 121-133.

2.   Xu, H.; Chen, R.; Sun, Q.; Lai, W.; Su, Q.; Huang, W.; Liu, X., Recent Progress in Metal-Organic Complexes for Optoelectronic Applications. *Chem. Soc. Rev.* **2014,** *43*, 3259-3302.

3.   Cebrian, C.; Mauro, M., Recent Advances in Phosphorescent Platinum Complexes for Organic Light-Emitting Diodes. *Beilstein J. Org. Chem.* **2018,** *14*, 1459-1481.

4.   Kim, H. U.; Jang, H. J.; Choi, W.; Kim, M.; Park, S.; Park, T.; Lee, J. Y.; Bejoymohandas, K. S., Ancillary Ligand-Assisted Robust Deep-Red Emission in Iridium(III) Complexes for Solution-Processable Phosphorescent OLEDs. *J. Mater. Chem. C.* **2019,** *7*, 4143-4154.

5.   Yersin, H.; Rausch, A. F.; Czerwieniec, R.; Hofbeck, T.; Fischer, T., The triplet State of Organo-Transition Metal Compounds. Triplet Harvesting and Singlet Harvesting for Efficient OLEDs. . *Coord. Chem. Rev.* **2011,** *255*, 2622-2652.

6.   Williams, J. a. G., *Photochemistry and Photophysics of Coordination Compounds II*. Springer:Berlin: 2007.

7.   Fleetham, T.; Li, G.; Li, J., Phosphorescent Pt(II) and Pd(II) Complexes for Efficient High-Color-Quality and Stable OLEDs. *Adv. Mater.* **2017,** *29*, 1601861.

8.   Farinola, G. M.; Ragni, R., Electroluminescent Materials for White Organic Light Emitting Diodes. *Chem. Soc. Rev* **2011,** *40*, 3467.

9.   Farinola, G. M.; Ragni, R., Organic Emitters for Solid State Lighting. *J. Solid State Light.* **2015,** *2*, 1.

10.   Xiao, L.; Chen, Z.; Qu, B.; Luo, J.; Kong, S.; Gong, Q.; Kido, J., Recent Progresses on Materials for Electrophosphorescent Organic Light-Emitting Devices. *Adv. Mater.* **2011,** *23*, 926-952.

11.   Herberger, J.; Winter, R. F., Platinum Emitters with Dye-Based σ-Aryl Ligands. *Coord. Chem. Rev.* **2019,** *400*, 213048.

12.   Strassner, T., Phosphorescent Platinum(II) Complexes with C∧C* Cyclometalated NHC Ligands. *Acc. Chem. Res.* **2016,** *49*, 2680-2689.

13.   Soellner, J.; Strassner, T., The "Enders Triazole" Revisited: Highly Efficient, Blue Platinum(II) Emitters. *Organometallics* **2018,** *37*, 1821- 1824.

14.   Pinter, P.; Unger, Y.; Strassner, T., Cyclometalated NHC Platinum(II) Complexes with Bridging Pyrazolates: Enhanced Photophysics of Binuclear Blue Emitters. *ChemPhotoChem* **2017,** *1*, 113-115.

15.   Tenne, M.; Metz, S.; Wagenblast, G.; Münsterb, I.; Strassner, T., C^C* Cyclometalated Platinum(II) N-Heterocyclic Carbene Complexes with a Sterically Demanding β-diketonato Ligand – Synthesis, Characterization and Photophysical properties. *Dalton Trans.* **2015,** *44*, 8444-8455.

16.   Ogawa, T.; Sameera, W. M. C.; Saito, D.; Yoshida, M.; Kobayashi, A.; Kato, M., Phosphorescence Properties of Discrete Platinum(II) Complex Anions Bearing N-Heterocyclic Carbenes in the Solid State. *Inorg.Chem.* **2018,** *57*, 14086-14096.

17.   Ko, S.-B.; Park, H.-J.; Gong, S.; Wang, X. N.; Lu, Z.-H.; Wang, S. N., Blue Phosphorescent N-Heterocyclic Carbene Chelated Pt(II) Complexes with an α-Duryl-β-Diketonato Ancillary Ligand. *Dalton Trans.* **2015,** *44*, 8433-8443.

18.　　Hudson, Z. M.; Sun, C.; Helander, M. G.; Chang, Y. L.; Lu, Z. H.; Wang, S. N., Highly Efficient Blue Phosphorescence from Triarylboron-Functionalized Platinum(II) Complexes of N-Heterocyclic Carbenes. *J. Am. Chem. Soc* **2012,** *134*, 13930-13933.

19.　　Arnal, L.; Fuertes, S.; Martin, A.; Sicilia, V., The Use of Cyclometalated NHCs and Pyrazoles for the Developement of Fully Efficient Blue Pt(II) Emitters and Pt/Ag Clusters. *Chem. Eur. J.* **2018,** *24*, 9377-9384.

20.　　Fuertes, S.; Chueca, A. J.; Arnal, L.; Martín, A.; Giovanella, U.; Botta, C.; Sicilia, V., Heteroleptic Cycloplatinated N-heterocyclic Carbene Complexes: A New Approach to Highly Efficient Blue-Light Emitters. *Inorg. Chem.* **2017,** *56*, 4829-4839.

21.　　Sicilia, V.; Fuertes, S.; Chueca, A. J.; Arnal, L.; Martín, A.; Perálvarez, M.; Botta, C.; Giovanella, U., Highly Efficient Platinum-Based Emitters for Warm White Light Emitting Diodes. *J. Mater. Chem. C.* **2019,** *7*, 4509-4516.

22.　　Fuertes, S.; Chueca, A. J.; Martín, A.; Sicilia, V., New NHC Cycloplatinated Compounds. Significance of the Cyclometalated Group on the Electronic and Emitting Properties of Biscyanide Compounds. *J. Organomet. Chem.* **2019,** *889*, 53-61.

23.　　Rausch, A. F.; Murphy, L.; Williams, J. A. G.; Yersin, H., Improving the Performance of Pt(II) Complexes for Blue Light Emission by Enhancing the Molecular Rigidity. *Inorg. Chem.* **2012,** *51*, 312-319.

24.　　Mi, B. X.; Wang, P. F.; Gao, Z. Q.; Lee, C. S.; Lee, S. T.; Hong, H. L.; Chen, X. M.; Wong, M. S.; Xia, P. F.; Cheah, K. W.; Chen, C. H.; Huang, W., Strong Luminescent Iridium Complexes with C^N—NStructure in Ligands and Their Potential in Efficient andThermally Stable Phosphorescent OLEDs. *Adv. Mater.* **2009,** *21*, 339-343.

25.　　Walden, M. T.; Pander, P.; Yufit, D. S.; Dias, F. B.; Williams, J. A. G., Homoleptic Platinum(II) Complexes with Pyridyltriazole Ligands: Excimer-Forming

Phosphorescent Emitters for Solution-Processed OLEDs. *J. Mater. Chem. C,* **2019,** *7,* 6592-6606.

26. Lam, E. S. H.; Tsang, D. P. K.; Lam, W. H.; Tam, A. Y. Y.; Chan, M. Y.; Wong, W. T.; Yam, V. W. W., Luminescent Platinum(II) Complexes of 1,3-Bis(N-alkylbenzimidazol2'-yl)benzene-Type Ligands with Potential Applications in Efficient Organic Light-Emitting Diodes. *Chem. - Eur. J.* **2013,** *19,* 6385-6397.

27. Liu, C.; Gu, Y.; Fu, Q.; Sun, N.; Zhong, C.; Ma, D.; Qin, J.; Yang, C., Nondoped Deep-Blue Organic Light-Emitting Diodes with Color Stability and Very Low Efficiency Roll-Off: Solution-Processable Small-Molecule Fluorophores by Phosphine Oxide Linkage. *Chem. - Eur. J.* **2012,** *18,* 13828-13835.

28. Cebrián, C.; Mauro, M.; Kourkoulos, D.; Mercandelli, P.; Hertel, D.; Meerholz, K.; Strassert, C. A.; De Cola, L., Luminescent Neutral Platinum Complexes Bearing an Asymmetric N ^N ^N Ligand for High-Performance Solution-Processed OLEDs. *Adv. Mater.* **2013,** *25,* 437-442.

29. Cheng, G.; Chen, Y.; Yang, C.; Lu, W.; Che, C. M., Highly Efficient Solution-Processable Organic Light-Emitting Devices with Pincer-Type Cyclometalated Platinum(II) Arylacetylide Complexes. *Chem. - Asian J.* **2013,** *8,* 1754-1759.

30. Cheng, G.; Chow, P. K.; Kui, S. C. F.; Kwok, C. C.; Che, C. M., High-Efficiency Polymer Light-Emitting Devices with Robust Phosphorescent Platinum(II) Emitters Containing Tetradentate Dianionic O ^ N ^ C ^ N Ligands *Adv. Mater.* **2013,** *25,* 6765-6770.

31. Lam, E. S. H.; Tam, A. Y. Y.; Chan, M. Y.; Yam, V. W. W., A New Class of Luminescent Platinum(II) Complexes of 1,3-Bis(N-alkylbenzimidazol-2'-yl)benzene-Type

Ligands and Their Application Studies in the Fabrication of Solution-Processable Organic Light-Emitting Devices. *Isr. J. Chem.* **2014,** *54*, 986-992.

32.   Li, H.; Li, J.; Ding, J. Q.; Yuan, W.; Zhang, Z. L.; Zou, L. Y.; Wang, X. D.; Zhan, H. M.; Xie, Z. Y.; Cheng, Y. X.; Wang, L. X., Design, Synthesis, and Optoelectronic Properties of Dendrimeric Pt(II) Complexes and Their Ability to Inhibit Intermolecular Interaction. *Inorg. Chem.* **2014,** *53*, 810-821.

33.   Li, Y.; Tsang, D. P. K.; Chan, C. K. M.; Wong, K. M. C.; Chan, M. Y.; Yam, V. W. W., Synthesis of Unsymmetric Bipyridine–Pt[II]–Alkynyl Complexes through Post-Click Reaction with Emission Enhancement Characteristics and Their Applications as Phosphorescent Organic Light-Emitting Diodes. *Chem. - Eur. J.* **2014,** *20*, 13710-13715.

34.   Kong, F. K.-W.; Tang, M.-C.; Wong, Y.-C.; Chan, M.-Y.; Yam, V. W.-W., Design   Strategy   for   High-Performance   Dendritic   Carbazole-Containing Alkynylplatinum(II) Complexes and Their Application in Solution-Processable Organic Light-Emitting Devices. *J. Am. Chem. Soc.* **2016,** *138*, 6281-6291.

35.   Kong, F. K.-W.; Tang, M.-C.; Wong, Y.-C.; Ng, M.; Chan, M.-Y.; Yam, V. W.-W., Strategy for the Realization of Efficient Solution-Processable Phosphorescent Organic Light-Emitting Devices: Design and Synthesis of Bipolar Alkynylplatinum(II) Complexes. *J. Am. Chem. Soc.* **2017,** *139*, 6351-6362.

36.   Hao, Z.; Meng, F.; Wang, P.; Wang, Y.; Tan, H.; Pei, Y.; Su, S.; Liu, Y., Dual Phosphorescence   Emission   of   Dinuclear   Platinum(II)   Complex   Incorporating Cyclometallating Pyrenyl-dipyridine-based Ligand and its Application in Near-infrared Solution-processed Polymer Light-Emitting Diodes. *Dalton Trans.* **2017,** *46*, 16257-16268.

37.   Okamura, N.; Egawa, K.; Maeda, T.; Yagi, S., Control of Excimer Phosphorescence by Steric Effects in Cyclometalated Platinum(II) Diketonate Complexes

Bearing Peripheral Carbazole Moieties towards Application in non-doped White OLEDs. *New J. Chem.* **2018,** *42*, 11583-11592.

38.   Yang, X.; Jiao, B.; Dang, J.-S.; Sun, Y.; Wu, Y.; Zhou, G.; Wong, W.-Y., Achieving High-Performance Solution-Processed Orange OLEDs with the Phosphorescent Cyclometalated Trinuclear Pt(II) Complex. *ACS App. Mat. Interfaces* **2018,** *10*, 10227-10235.

39.   Zhao, J.; Feng, Z.; Zhong, D.; Yang, X.; Wu, Y.; Zhou, G.; Wu, Z., Cyclometalated Platinum Complexes with Aggregation-Induced Phosphorescence Emission Behavior and Highly Efficient Electroluminescent Ability. *Chem. Mater.* **2018,** *30*, 929-946.

40.   Shafikov, M. Z.; Daniels, R.; Pander, P.; Dias, F. B.; Williams, J. A. G.; Kozhevnikov, V. N., Dinuclear Design of a Pt(II) Complex Affording Highly Efficient Red Emission: Photophysical Properties and Application in Solution-Processible OLEDs. *ACS App. Mat. Interfaces* **2019,** *11*, 8182-8193.

41.   Fuertes, S.; Chueca, A. J.; Sicilia, V., Exploring the Transphobia Effect on Heteroleptic NHC Cycloplatinated Complexes. *Inorg. Chem.* **2015,** *54*, 9885-9895.

42.   Fuertes, S.; Chueca, A. J.; Perálvarez, M.; Borja, P.; Torrell, M.; Carreras, J.; Sicilia, V., White Light Emission from Planar Remote Phosphor Based on NHC Cycloplatinated Complexes. *ACS Appl. Mater. Interfaces* **2016,** *8*, 16160-16169.

43.   Fuertes, S.; García, H.; Perálvarez, M.; Hertog, W.; Carreras, J.; Sicilia, V., Stepwise Strategy to Cyclometallated Pt[II] Complexes with N-Heterocyclic Carbene Ligands: A Luminescence Study on New β-Diketonate Complexes. *Chem. -Eur. J.* **2015,** *21*, 1620-1631.

44.   Unger, Y.; Meyer, D.; Molt, O.; Schildknecht, C.; Münster, I.; Wagenblast, G.; Strassner, T., Green-Blue Emitters: NHC-Based Cyclometalated [Pt(C^C*)(acac)] Complexes. . *Angew. Chem., Int. Ed.* **2010,** *49*, 10214-10216.

45.   Diez, A.; Fornies, J.; Fuertes, S.; Lalinde, E.; Larraz, C.; Lopez, J. A.; Martin, A.; Moreno, M. T.; Sicilia, V., Synthesis and Luminescence of Cyclometalated Compounds with Nitrile and Isocyanide Ligands. *Organometallics* **2009,** *28*, 1705-1718.

46.   Graber, S.; Doyle, K.; Neuburger, M.; Housecroft, C. E.; Constable, E. C.; Costa, R. D.; Orti, E.; Repetto, D.; Bolink, H. J., A Supramolecularly-Caged Ionic Iridium(III) Complex Yielding Bright and Very Stable Solid-State Light-Emitting Electrochemical Cells. *J. Am. Chem. Soc.,* **2008,** *130*, 14944-14945.

47.   Jude, H.; Rein, F. N.; White, P. S.; Dattelbaum, D. M.; Rocha, R. C., Synthesis, Structure, and Electronic Properties of a Dimer of Ru(bpy)$_2$ Doubly Bridged by Methoxide and Pyrazolate. *Inorg. Chem.* **2008,** *47*, 7695-7702.

48.   Geary, W. J., The Use of Conductivity Measurements in Organic Solvents for the Characterisation of Coordination Compounds. *Coord. Chem Rev* **1971,** *7*, 81-122.

49.   Haneder, S.; Da Como, E.; Feldmann, J.; Lupton, J. M.; Lennartz, C.; Erk, P.; Fuchs, E.; Molt, O.; Münster, I.; Schildknecht, C.; Wagenblast, G., Controlling the Radiative Rate of Deep-Blue Electrophosphorescent Organometallic Complexes by Singlet-Triplet Gap Engineering. *Adv. Mater.* **2008,** *20*, 3325-3330.

50.   Tsuboyama, A.; Iwawaki, H.; Furugori, M.; Mukaide, T.; Kamatani, J.; Igawa, S.; Moriyama, T.; Miura, S.; Takiguchi, T.; Okada, S.; Hoshino, M.; Ueno, K., Homoleptic Cyclometalated Iridium Complexes with Highly Efficient Red Phosphorescence and Application to Organic Light-Emitting Diode. *J. Am. Chem. Soc* **2003,** *125*, 12971-12979.

51.	Fleetham, T.; Wang, Z.; Li, J., Efficient Deep Blue Electrophosphorescent Devices Based on Platinum(II) bis(n-methyl-imidazolyl)benzene Chloride. *Org. Electron.,* **2012,** *13*, 1430-1435.

52.	Hang, X.-C.; Fleetham, T.; Turner, E.; Brooks, J.; Li, J., Highly Efficient Blue-Emitting Cyclometalated Platinum(II) Complexes by Judicious Molecular Design. *Angew. Chem., Int. Ed.* **2013,** *52*, 6753-6756.

53.	Jou, J.-H.; Peng, S.-H.; Chiang, C.-I.; Chen, Y.-L.; Lin, Y.-X.; Jou, Y.-C.; Chen, C.-H.; Li, C.-J.; Wang, W.-B.; Shen, S.-M.; Chen, S.-Z.; Wei, M.-K.; Sun, Y.-S.; Hung, H.-W.; Liu, M.-C.; Lin, Y.-P.; Li, J.-Y.; Wang, C.-W., High Efficiency Yellow Organic Light-Emitting Diodes with a Solution-Processed Molecular Host-based Emissive Layer. *J. Mater. Chem. C,* **2013,** *1*, 1680-1686.

FOR TABLE OF CONTENTS ONLY

Highly photoluminescent ionic platinum-based emitters, [Pt(R-C^C*)(P^P)]PF$_6$, were prepared. They show an efficient blue or cyan emission in PMMA films (5%wt), with PLQY ranging from 30% to 87%. Solution processed OLEDs based on **3A** and **3B** show CIE coordinates (0.22, 0.41 **3A**; 0.24, 044 **3B**) fitting within the sky blue region.